

# Cholec80-port: A Geometrically Consistent Trocar Port Segmentation Dataset for Robust Surgical Scene Understanding

Shunsuke Kikuchi<sup>1</sup> Atsushi Kouno<sup>1</sup> Hiroki Matsuzaki<sup>1</sup>

<sup>1</sup>Jmees Inc., Kashiwa-city, Chiba, Japan

[engineer@jmees-inc.com](mailto:engineer@jmees-inc.com)

**Keywords:** trocar port; semantic segmentation; dataset; data cleansing; geometric consistency

## 1 Introduction

Precise segmentation of surgical instruments and anatomical structures is essential for advanced surgical scene understanding. Beyond recognition, many downstream geometry-based tasks require robust separation of local motion (dynamic objects) from global motion (anatomical background), including image stitching, 3D reconstruction, and visual SLAM (vSLAM). Prior work has shown that masking dynamic regions during feature extraction can improve geometric pipelines by preventing trackers from following moving outliers [1].

In laparoscopic surgery, the trocar port serves as the physical gateway through the abdominal wall. Because the endoscopic camera passes through these ports, they can obstruct the field of view. While ports are most visible during camera insertion and retraction, they may remain partially visible throughout procedures as peripheral or even central occlusions. Importantly, port surfaces are often specular and textured, attracting an excessive number of feature points. Unlike surgical instruments, ports are approximately camera-fixed and persist over long durations, making them uniquely detrimental to geometry-based methods: they repeatedly introduce strong, non-anatomical features that can bias matching, increase geometric error, and cause alignment artifacts.

Despite this utility, explicit port labels are conspicuously absent from most large-scale datasets. This scarcity is largely attributed to de-identification concerns, because ports can capture transitions to the exterior environment; consequently, ports are frequently merged into broader categories (e.g., “abdominal wall” in related datasets).

Currently, only two public datasets, m2caiSeg [2] and GynSurg [3], provide explicit labels for “trocars” or “cannulas”. However, both contain limitations for geometry-aware applications. m2caiSeg is small ( $N=370$ ) and exhibits annotation artifacts (e.g., interpolation noise). GynSurg is larger ( $N=4873$ ), but its COCO polygon representation can induce a “hole-filling” policy in which the central lumen is masked, which is geometrically inconsistent when organs are visible through the opening. To address these limitations, we propose Cholec80-port<sup>1</sup> Our contributions are:

1. A rigorous and practical annotation SOP that prioritizes geometric fidelity by defining a port-sleeve mask that excludes the central opening.
2. A large-scale dataset from Cholec80 and data cleansing of existing datasets to unify them under the proposed SOP.
3. A pretrained baseline port segmentation model released with tooling to support downstream surgical computer vision research.

---

<sup>1</sup>Dataset and Source code is available at <https://github.com/JmeesInc/cholec80-port>

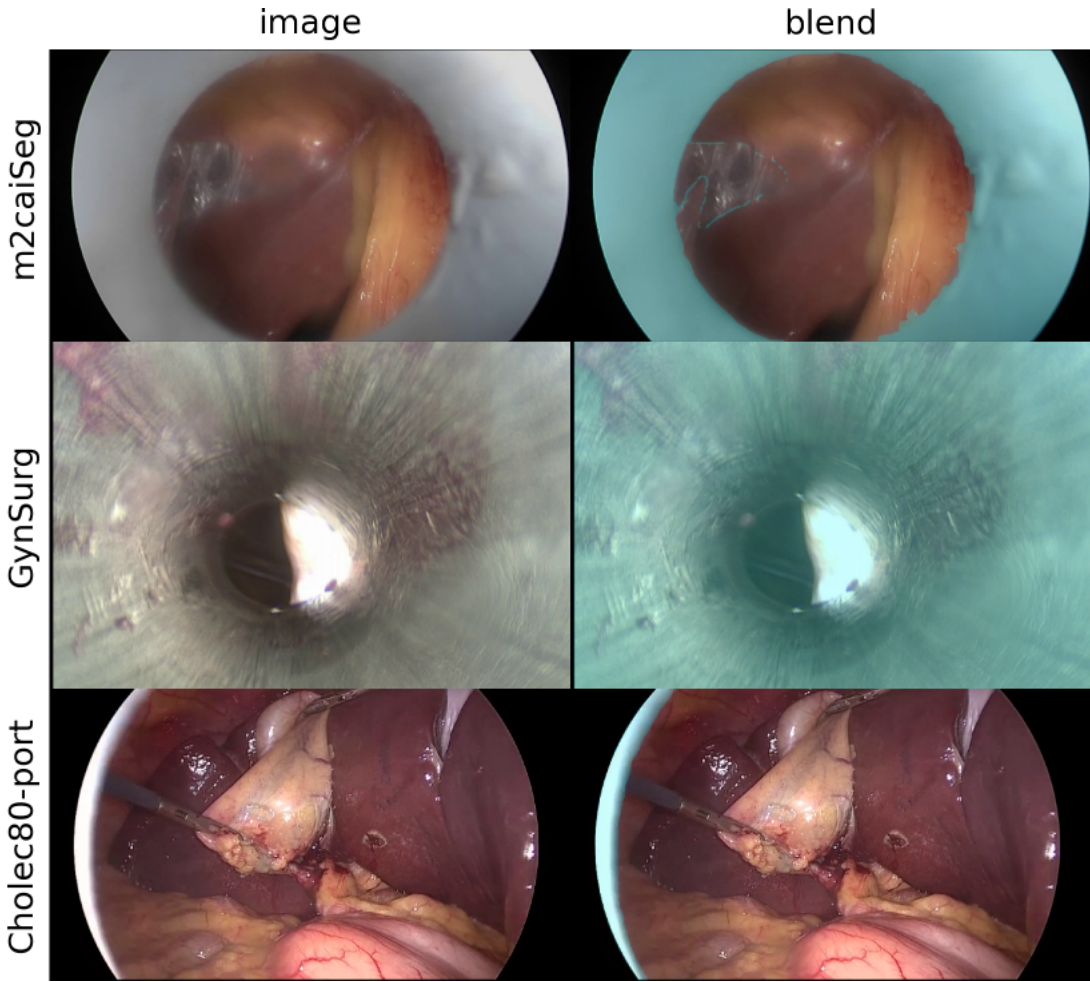


Figure 1: **Annotation consistency.** Examples of erroneous labels in m2caiSeg (top) and GynSurg (middle) and the proposed geometrically consistent port-sleeve labels in Cholec80-port (bottom). For each row, the original frame (left) and an overlay visualization (right) are shown.

## 2 Methods

### 2.1 Dataset acquisition and sampling

We utilized the first 20 videos from Cholec80. To balance surgical scene diversity with annotation efficiency, we sampled every 30 frames, resulting in 38,434 annotated frames. The dataset was split at the video level to avoid leakage: Videos 01–08 for training, 09–10 for validation, and 11–20 for testing.

Among sampled frames, 1,398 frames contain visible ports. This yields a substantially larger positive sample size than m2caiSeg ( $n=255$ ) and GynSurg ( $n=130$ ), improving robustness for both segmentation and detection-like use cases.

### 2.2 Annotation SOP: port-sleeve definition

All annotations were performed using CVAT [4]. We define the target region as the sleeve: the rigid metallic or plastic cylindrical component visible beyond the internal valve. Crucially, the sleeve definition **excludes** the central lumen (opening), because masking the lumen can suppress anatomically valid pixels and introduce geometric inconsistencies for image-plane aggregation and feature extraction.

For ambiguous frames where boundaries are unclear due to orientation or specular highlights, we consulted

Table 1: **Port segmentation results (Dice and Detect F1).** Rows denote the training dataset; columns denote the evaluation dataset. Dice is computed only on port-present frames (GT> 0).

Train data	m2caiSeg (test)		GynSurg (Video 09–10)		Cholec80-port (test)	
	Dice (GT> 0)	Detect F1	Dice (GT> 0)	Detect F1	Dice (GT> 0)	Detect F1
m2caiSeg (train)	0.4477 $\pm$ 0.4477	0.6667	0.0029 $\pm$ 0.0027	0.0294	0.2485 $\pm$ 0.3785	0.2949
GynSurg (Video 01–08)	0.3274 $\pm$ 0.3274	0.6667	0.8800 $\pm$ 0.0920	0.8529	0.3258 $\pm$ 0.3789	0.6053
Cholec80-port (train)	0.4876 $\pm$ 0.4876	0.6667	0.6110 $\pm$ 0.0637	0.5588	0.8616 $\pm$ 0.1216	0.8556
Combined (cleaned)	0.7218 $\pm$ 0.2610	1.0000	0.8185 $\pm$ 0.0840	0.8235	0.8127 $\pm$ 0.3057	0.8698

temporal context (neighboring frames) to confirm the physical extent of the sleeve. This temporal verification helps distinguish sleeve boundaries from transient reflections and motion blur.

### 2.3 Cleansing and unification of existing datasets

We additionally cleanse and unify existing datasets under the same SOP:

- m2caiSeg: We re-annotated the dataset to remove interpolation artifacts and spurious masks. After cleansing, only a small subset satisfies the proposed high-quality, sleeve-consistent criteria.
- GynSurg: We corrected the hole-filling issue by segmenting central lumen regions and subtracting them from the original polygons to derive sleeve-only masks.

### 2.4 Model and training protocol

We evaluate dataset efficacy using a ConvNeXt-Base [5] encoder with a U-Net [6] decoder for binary semantic segmentation. We train with a standard combined objective:

$$\mathcal{L} = \mathcal{L}_{\text{Dice}}(Y_{\text{pred}}, Y_{\text{true}}) + \mathcal{L}_{\text{BCE}}(Y_{\text{pred}}, Y_{\text{true}}). \quad (1)$$

Training uses AdamW [7] with learning rate  $5 \times 10^{-5}$ , batch size 16, and input resolution  $384 \times 384$ .

### 2.5 Evaluation metrics

We report two complementary metrics:

1. Dice score (segmentation fidelity): computed only on frames where ports are present (i.e.,  $\|Y_{\text{true}}\|_1 > 0$ ) to measure boundary recovery when the target exists.
2. Detect F1 (frame-level robustness): a frame is classified as positive if at least one pixel is predicted/annotated as port, and negative otherwise; we then compute F1 across frames.

To quantify the impact of SOP consistency and cleansing, we perform ablations using original (uncleaned) datasets under the same model and protocol.

## 3 Results

Table 1 summarizes performance across datasets. Training on Cholec80-port yields strong in-domain results on the Cholec80-port test split (Dice 0.862; Detect F1 0.856). Notably, the Cholec80-port-trained model also outperforms the m2caiSeg-trained model even when evaluated on the m2caiSeg test split, suggesting that geometrically consistent sleeve labels improve robustness beyond dataset-specific fitting.

Cross-dataset generalization to GynSurg remains challenging, likely due to domain shift in port materials, lighting, and surgical workflow. Even with a combined cleaned dataset, residual gaps indicate that visual diversity (e.g., transparent ports, boundary visibility, peripheral appearances) remains a key limiting factor.

Our cleansing of m2caiSeg indicates that many original labels are noisy under a sleeve-consistent definition; after re-annotation, only a small number of frames meet quality criteria, yielding high variance and limited

generalization. Ablations without cleansing (not shown) demonstrate substantially worse transfer, supporting the conclusion that SOP-level geometric consistency is a dominant factor for cross-dataset robustness.

Failure cases typically involve (i) faint ports near the image boundary, (ii) transparent/low-contrast sleeves with visible background through the structure, and (iii) strong specular highlights obscuring sleeve boundaries.

## 4 Conclusion

We presented Cholec80-port, a high-fidelity trocar port segmentation dataset derived from Cholec80, together with a geometrically consistent annotation SOP that defines port-sleeve masks excluding the central lumen. Experiments show that models trained on Cholec80-port achieve strong robustness and improved cross-dataset generalization compared with models trained on existing public data, and that rigorous cleansing can substantially improve transfer performance.

Domain shift across datasets remains a challenge, suggesting that additional diversity in port appearances and surgical environments is necessary for universal applicability. Future work will expand port segmentation coverage and integrate port masking into geometry-based pipelines such as vSLAM, 3D reconstruction, and panoramic inference.

## References

- [1] M. Hayoz, C. Hahne, T. Kurmann, M. Allan, G. Beldi, D. Candinas, P. Márquez-Neila, and R. Sznitman. Online 3d reconstruction and dense tracking in endoscopic videos. In *Medical Image Computing and Computer Assisted Intervention – MICCAI 2024*, volume 15006 of *Lecture Notes in Computer Science*, pages 444–454. Springer Nature Switzerland, October 2024.
- [2] S. Maqbool, A. Riaz, H. Sajid, and O. Hasan. m2caiseg: Semantic segmentation of laparoscopic images using convolutional neural networks. *arXiv preprint arXiv:2008.10134*, 2020.
- [3] S. Nasirihaghghi, N. Ghamsarian, L. Peschek, M. Munari, H. Husslein, R. Sznitman, and K. Schoemann. Gynsurf: A comprehensive gynecology laparoscopic surgery dataset. In *Proceedings of the ACM International Conference on Multimedia*, volume 33, pages 13141–13147, 2025.
- [4] Boris Sekachev, Nikita Manovich, Maxim Zhiltsov, Andrey Zhavoronkov, Dmitry Kalinin, Ben Hoff, TOsmanov, Dmitry Kruchinin, Artyom Zankevich, DmitriySidnev, Maksim Markelov, Johannes222, Mathis Chenuet, a andre, telenachos, Aleksandr Melnikov, Jijoong Kim, Liron Ilouz, Nikita Glazov, Priya4607, Rush Tehrani, Seungwon Jeong, Vladimir Skubrev, Sebastian Yonekura, vugia truong, zliang7, lizhming, and Tritin Truong. opencv/cvat: v1.1.0, August 2020.
- [5] Z. Liu, H. Mao, C.-Y. Wu, C. Feichtenhofer, T. Darrell, and S. Xie. A convnet for the 2020s. In *Proceedings of the IEEE/CVF Conference on Computer Vision and Pattern Recognition (CVPR)*, 2022.
- [6] O. Ronneberger, P. Fischer, and T. Brox. U-net: Convolutional networks for biomedical image segmentation. In *Medical Image Computing and Computer-Assisted Intervention – MICCAI 2015*, pages 234–241, 2015.
- [7] I. Loshchilov and F. Hutter. Decoupled weight decay regularization. In *International Conference on Learning Representations (ICLR)*, 2019.